Bent Strips in External Magnetic Fields and With Applied Currents

Leonardo R. E. Cabral and J. Albino Aguiar
Departamento de Física, Universidade Federal de Pernambuco,
50670 - 901 Recife, Brasil

Received on 28 February, 2002

Current and magnetic field profiles of bent strips in external magnetic fields and with applied currents are numerically calculated. The flat strip is correctly obtained as the limiting case of bent strips when the bend angle is zero. The Meissner response and the flux penetration are studied, the latter under the consideration of high critical currents and small bends. The dependence of these profiles on the creep exponent (by a material relation $E \propto (j/j_c)^n$) is also studied. In the presence of an external magnetic field the flux penetration is delayed in bent strips compared with flat strips. In the case of an applied current the flux penetration from the strip edge is also delayed, but a flux front starting from the corner is also observed.

I Introduction

The electromagnetic response of superconductors in external fields has been extensively studied, and special attention has been given to the role of the specimen shape. The Meissner state can be studied by London theory and is easily obtained in specimens with negligible demagnetization factor (long bars and cylinders in parallel fields). However, it turns out to be a difficult task when specimens with large and/or non-uniform demagnetization factors are considered in the perpendicular field geometry (in this case, the field is applied perpendicular to the specimen larger dimensions). In the limit where λ is much smaller than the sample dimensions, analytical solutions are known for a few cases, e.g., the Meissner response in perpendicular field in flat thin strips [1, 2] and disks [3, 4], long bars with elliptic [5] and rectangular cross-section [6].

The understanding of vortex penetration and evolution inside a type-II superconductor in the mixed state, can become a very difficult problem, due to the vortex-vortex and vortex-defects interactions, besides the influence of thermal fluctuations [7, 8]. At finite temperature vortices can be depinned from their preferential positions by thermal fluctuations. This generated motion of vortices, known as flux creep, induces an electric field,E, related to the current density, j, by $E(j) = E_c \exp(-U(j)/k_BT)$, where $U(j)$ is the pinning potential [10, 11].

The critical state approach can be used to study the way how magnetic flux evolves into the superconductor without carrying out the more fundamental London and Ginzburg-Landau theories. Again, for long superconducting bars and cylinders in parallel field geometry, the critical state is well understood. However, few analytical results are known for specimens in the so-called perpendicular geometry [1, 2, 9].

Although analytical results are important, numerical methods can be employed in order to obtain the Meissner response and the flux penetration into superconductors of several shapes [12, 13]. In this way Brandt formulated a numerical method which calculates the current density, j, inside cylinders and long bars (with finite aspect ratio) in external magnetic field or with applied currents [12, 14]. The magnetic field and the magnetization are also obtained from the calculated j. A material relation $E = E(j)$ also allows the investigation of flux creep effects, which are absent in the original critical state approach and are analytically calculated only in parallel field geometry.

In this work we present the eletromagnetic response of superconducting bent strips in external magnetic fields and with applied currents. The Meissner state and the flux penetration are obtained applying Brandt's method [12, 14] with the appropriate change of coordinates for bent strips. As a result points on the bent strip are described by a unique coordinate, ζ. The numerical calculated current and magnetic field profiles are also ζ dependent. The dependence of these profiles and of the magnetic moment on the bend angle is studied. The flux front coming from the strip edges is delayed for bent strips compared with flat ones, both in external magnetic fields or with an applied current. In the later case, however, a flux front coming from the bend is observed.

II Numerical method

The numerical method starts from the integral formulation of Ampère's law, Faraday's law and a relation $E = E(j)$ borrowed from microscopic theories about flux creep and flux flow. The external magnetic field is applied along the y-axis. The transport current results from an uniform external electric field along the z-axis. The current density, $\mathbf{j}$, the electric field, $\mathbf{E}$, and the vector potential, $\mathbf{A}$, are also assumed to be parallel to z-axis. This assumption is reasonable for long cilinders with symmetry axis along z-axis and arbitrary (uniform) cross-section in the $x-y$ plane. This leads to the following equation of motion for the current density,

$$\mu_0 \frac{\partial}{\partial t} j(\mathbf{r}) = -\int d^2r'\, Q^{-1}(\mathbf{r},\mathbf{r}')\left[E(j) + \frac{\partial}{\partial t} A_a\right], \quad (1)$$

where $\mathbf{j} = j\hat{z}$, $\mathbf{r} = (x, y)$, A_a is the vector potential of the applied field. For applied magnetic or electric fields, $A_a = -x\,B_a$ or $A_a = -\int dt\, E_a(t)$, respectively. The inverse kernel, $Q^{-1}(\mathbf{r},\mathbf{r}')$ can be obtained by the following identity,

$$\int d^2r''\, Q^{-1}(\mathbf{r}',\mathbf{r}'')\, Q(\mathbf{r}'',\mathbf{r}) = \delta(\mathbf{r}-\mathbf{r}'), \quad (2)$$

where $Q(\mathbf{r},\mathbf{r}')$ is the kernel relating the vector potential at a point $\mathbf{r}$ with the current density at all points inside the superconductor,

$$A(\mathbf{r}) = A_a + \mu_0 \int d^2r'\, Q(\mathbf{r},\mathbf{r}')\, j(\mathbf{r}'). \quad (3)$$

For long bars (long cylinders with rectangular cross-section) this kernel is obtained from the integration of the 3D kernel $1/(4*\pi|\mathbf{r}-\mathbf{r}'|)$ along the symmetry axis z, furnishing

$$\begin{aligned} Q_{\rm bar}(\mathbf{r},\mathbf{r}') &= -\frac{1}{4\pi}\ln\left[(x-x')^2+(y-y')^2\right] + \\ &+ \frac{1}{2\pi}\ln L, \end{aligned} \quad (4)$$

where L is the bar length along z. The Meissner response may be found by formula 1 taking $E = 0$ (no vortices present) and integrating in time. This yields

$$\mu_0\, j_M(\mathbf{r}) = -\int d^2r'\, Q^{-1}(\mathbf{r},\mathbf{r}')\, A_a. \quad (5)$$

We consider a thin bent strip, shown in Fig. 1, a thin strip sharply bent in the middle by an angle α, with thickness d and at $-a \le \zeta \le a$. Thus the strip cross-section is "V" shapep. The following change of coordinates,

$$\begin{aligned} x &= \zeta\cos\alpha - \mathrm{sign}(\zeta)\,\eta\,\mathrm{sen}\alpha \\ y &= |\zeta|\,\mathrm{sen}\alpha + \eta\cos\alpha, \end{aligned} \quad (6)$$

may be used into equation 4 in order to obtain the kernel for thin bent strips. Hence, Ampère's law can be written as

$$A(\zeta) = A_a + \mu_0 \int_{-a}^{a} d\zeta'\, Q(\zeta,\zeta')\, J_s(\zeta'), \quad (7)$$

where $J_s(\zeta) = \int_{-d/2}^{d/2} d\eta\, j(\zeta,\,\eta) \approx d\, j(\zeta)$ is the sheet current (the current density integrated over the thickness) and the kernel $Q(\zeta,\zeta')$ is given by

$$\begin{aligned} Q(\zeta,\zeta') &= -\frac{1}{4\pi}\ln\left[(\zeta-\zeta')^2\cos^2\alpha + (|\zeta|-|\zeta'|)^2\mathrm{sen}^2\alpha\right] + \\ &+ \frac{1}{2\pi}\ln L. \end{aligned} \quad (8)$$

The vector potential of the external fields is $A_a = -\zeta\cos\alpha\, B_a$, for an external magnetic field $\mathbf{B}_a$, or $A_a = -\int dt\, E_a$ for an applied electric field. Notice that the dependence on the coordinate η – along the thickness – is dropped out, since we consider thin bent strips. This leads to an equation of motion for the sheet current

$$\mu_0 \frac{\partial}{\partial t} J_s(\zeta) = -\int_{-a}^{a} d\zeta'\, Q^{-1}(\zeta,\zeta')\left[E\Big(\frac{J_s}{D}\Big) + \frac{\partial}{\partial t} A_a\right], \quad (9)$$

and to the sheet current for the Meissner state

$$\mu_0\, J_s^M(\zeta) = -\int d\zeta'\, Q^{-1}(\zeta,\zeta')\, A_a \quad (10)$$

where the inverse kernel is found similarly to eq. 4 for the bar, but integrating over ζ, i.e.,

$$\int d\zeta''\, Q^{-1}(\zeta',\zeta'')\, Q(\zeta'',\zeta) = \delta(\zeta-\zeta'). \quad (11)$$

By discretizing the coordinate along the bent strip, ζ, one can numerically solve the above equation for the Meissner response and integrate the equation of motion for J_s.

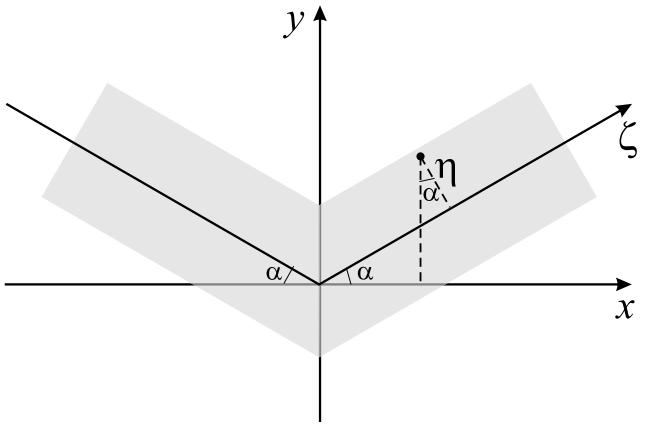

Figure 1. Schematic picture of a bent strip. The thickness is magnified in order to better visualization. The coordinate along the strip is ζ and the direction perpendicular to ζ is denoted by η.

In the calculations the following symmetry relations for J_s were used: in external magnetic (along

y) or electric (along z) fields, $J_s(-\zeta) = -J_s(\zeta)$ or $J_s(-\zeta) = J_s(\zeta)$, respectively. Thus the above integral ranges from 0 to a allowing for greater accuracy. Hence, the kernel (eq. 8) becomes,

$$Q^B(\zeta,\zeta') = -\frac{1}{4\pi}\ln\left[\frac{\zeta_-^2}{\zeta_+^2\cos^2\alpha + \zeta_-^2\sin^2\alpha}\right], \qquad (12)$$

for an applied $\mathbf{B}_a = B_a\hat{y}$ and

$$Q^I(\zeta,\zeta') = -\frac{1}{4\pi}\ln\left\{\frac{\zeta_-^2[\zeta_+^2\cos^2\alpha + \zeta_-^2\sin^2\alpha]}{L^4}\right\}. \qquad (13)$$

for $\mathbf{E}_a = E_a\hat{z}$ (equivalent to apply a transport current), where $\zeta_\pm = \zeta \pm \zeta'$. When an external and a transport current are present, the kernel given by equation 8 should be used.

The magnetic field is obtained from the curl of $\mathbf{A}$, which reads

$$\mathbf{B} = \hat{\eta}B_\eta = \nabla\times\mathbf{A} = \hat{\eta}\,B_a\cos\alpha - \hat{\eta}\,\frac{\partial A_J}{\partial\zeta}, \qquad (14)$$

where $\hat{\eta}$ is a unit vector parallel to the coordinate η. For the case of an external magnetic field (no applied current) the magnetic moment is found from the following formula

$$\mathbf{m} = \frac{1}{2}\int d^3r\ \mathbf{r}\times\mathbf{j} = -\hat{y}\,2L\,d\cos\alpha\int_0^a d\zeta\ \zeta\ J_s(\zeta). \qquad (15)$$

In this equation it is considered the contribution to the magnetization from the U-turning currents near the strip ends, at $|z| \approx L/2$ [2]. When an applied electric field is present,

$$I = 2\int_0^a d\zeta\ J_s(\zeta). \qquad (16)$$

gives the total current flowing through the bent strip.

We chose a grid of $N = 100$ points to represent half of the bent strip (i.e., $0 \le \zeta \le a$). It was also adopted $d = 2.5\times10^{-4}\,a$. In this way ζ, $J_s(\zeta)$ and $B_\eta(\zeta)$ become one dimensional arrays, and the kernel $Q(\zeta,\zeta')$ becomes a square matrix. Hence the integrals shown above are converted into sums over the index of these arrays and the inverse kernel $Q^{-1}(\zeta,\zeta')$ can be computed by matrix inversion.

III Results

The calculated magnetic field lines for the Meissner response are depicted in Figs. 2 and 3, the former for an external magnetic field $B_a\|\hat{y}$ and the latter for a transport current (which is the same as applying an electric field parallel to $\hat{z}$). Bend angles $\alpha = 0^o$, 30^o, 60^o and 90^o are shown. The magnetic field lines are obtained from the equipotencial lines of the vector potencial, $\mathbf{A}$. For the external magnetic field case the magnetic field lines tend to be uniform as the distance from the strip increase. For the transport current, the magnetic field lines circulate around the strips, becoming more spaced farther from the strip. In both cases it is observed that the magnetic field lines bend sharply at the edges. These lines are also not allowed to enter the strips as expected in the Meissner state. The case $\alpha = 90^o$ correctly results in flat with width a [half of the width $(2a)$ for a flat strip, when $\alpha = 0^o$]. Interestingly, in the cases $0^o < \alpha < 90^o$ the magnetic flux is shielded in the inner wedge of the bent strip.

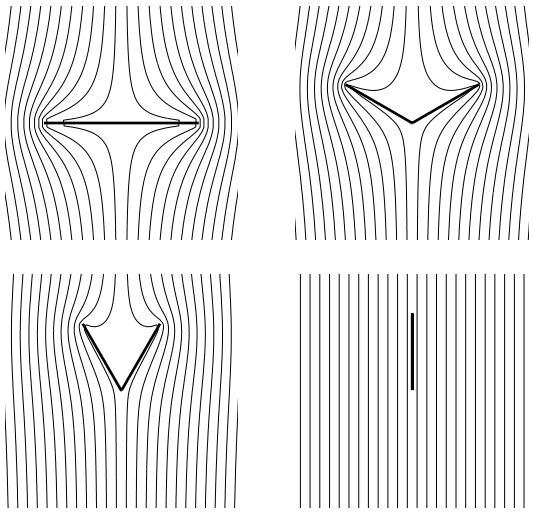

Figure 2. Magnetic field lines for bent thin strips in an external field $B_a\|\hat{y}$. Four bend angles are shown: $\alpha = 0^o$, corresponding to a flat strip, (top left); $\alpha = 30^o$ (top right); $\alpha = 60^o$ (bottom left) and $\alpha = 90^o$ (bottom right).

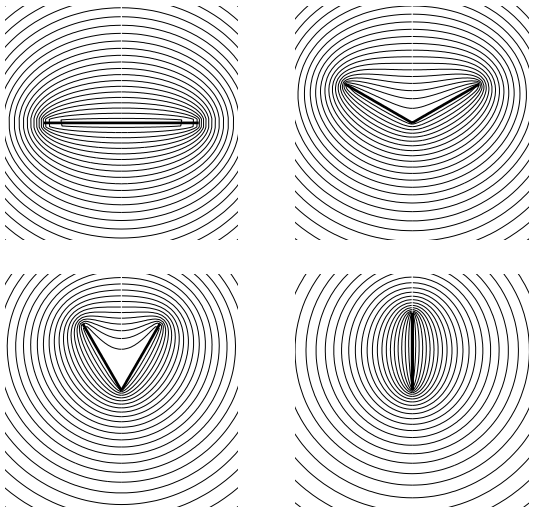

Figure 3. The same as Fig. 2, but for a transport current flowing along $\hat{z}$.

The flux penetration is presented in the Figs 4 and 5 for an external magnetic field and for a transport current, respectively. The magnetic field profiles are depicted in the top and the current profiles in the bottom

of the figures. Because of the symmetry of the profiles (the magnetic component, B_η, and the sheet current, J_s, are, respectively, even and odd functions of ζ for an external magnetic field, while B_η and J_s are odd and even functions of ζ for the transport current case), the figures show the $\zeta > 0$ branch only. The Bean critical state assumption (j_c = constant) [15] was considered in all cases treated in this article. In the external field case the increasing and decreasing branches are shown in the left and right of the Fig. 4 for $n = 101$. The continuous (dashed) line presents the profiles taken from the $\alpha = 0^0$ ($\alpha = 30^0$) case.

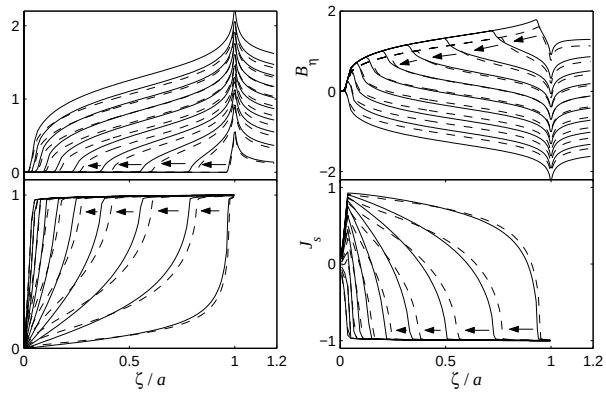

Figure 4. Sheet current, J_s, (bottom) and the perpendicular component of the induction, B_η, (top) dependence on the coordinate parallel to the bent strip, ζ, for bent strips in external magnetic fields. **Left**: increasing branch. **Right**: decreasing branch. The thin and dashed correspond to $\alpha = 0^o$ and 30^o, respectively. Each group of two profiles, indicated by the arrows, are obtained at the same external field. J_s and B_η/μ_0 are in units of $j_c\, D$, and we used $d = 2{,}5 \times 10^{-4}\, a$. Notice that J_s and B_η are, respectively, odd and even functions on ζ.

The profiles for these two bend angles were calculated for the same external fields, where the arrows indicate the direction in which the external field increases. The divergence of the magnetic field at the strip edge $\zeta = a$, which had already been obtained for a flat strip ($\alpha = 0^o$) [1, 2, 9], is also observed when $\alpha > 0^o$. As the external field increases, magnetic flux penetrates deeper into the strip, and the shielded region becomes narrower. The difference between the $\alpha = 0^o$ and $\alpha = 30^o$ cases appear as a delayed penetration in the later case. In fact, the penetration is more delayed as the bend angle increases [16]. In the region the flux has penetrated, the sheet current is almost constant, as expected for the Bean critical state (the small deviation from the constant value occurs due to the finite creep exponent, $n = 101$). J_s decreases towards zero, in the shielded region, as one walks to the middle of the strip, although the decays for $\alpha = 0^o$ and $\alpha = 30^o$ present different behaviors. For each external field, there is a crossover separating a region where $J_s(0^o) > J_s(30^o)$ from the region where $J_s(0^o) < J_s(30^o)$. In the decreasing branch the same features observed in increasing branch are obtained. The difference comes from the fact that flux starts to leave the strip through the edges $\zeta = \pm a$ and a region where magnetic flux is trapped appears.

In the transport current case the profiles were obtained at increasing time, keeping an uniform electric field in the $\hat{z}$ constant (Fig. 5). This makes the total current (which is the applied current) flowing in the strip increase with time. The thin dashed, dash-dotted and thick lines represent the bend angles $\alpha = 0^o$, 15^o, 30^o and 45^o, respectively. Each group of four profiles, indicated by the arrows, are obtained at the same time (or, for the same transport current). In the left(right), $n = 101 (n = 11)$ was adopted, corresponding to weak (strong) flux creep. The influence of creep is evidenciated by the smoother profiles and the larger flux diffusion into the strip for $n = 11$ compared with $n = 101$. For both cases the flux penetration from the strip edges $\zeta = \pm a$ is more delayed as the bend angle increases. However, a new feature is observed: flux penetrates from the middle of the bent strip, at $\zeta = 0$, where the strip bends. This does not happen for a flat strip and occurs in bent strips because of the nonzero perpendicular magnetic field component at the bend (see Fig. 3). This penetration is more pronounced for larger α values. After the critical current is attained the sheet current becomes uniform through the strip [2], which corresponds to the full flux penetration. This is depicted in the last profile in the right of Fig. 5 (although it is not shown in the left of this figure, this stage is also present for $n = 101$).

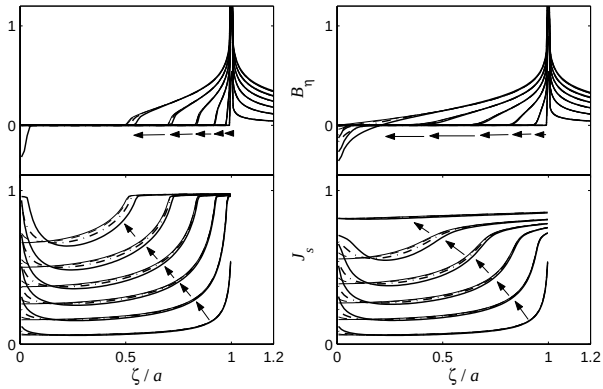

Figure 5. Sheet current, J_s, (bottom) and the perpendicular component of the induction, B_η, (top) dependence on the coordinate parallel to the bent strip, ζ, for bent strips with an uniform electric field. **Left**: $n = 101$. **Right**: $n = 11$. The thin, dashed, dash-dotted and thick lines correspond to $\alpha = 0^o$, 15^o, 30^o and 45^o, respectively. Each group of four profiles, indicated by the arrows, are obtained at the same time. J_s and B_η/μ_0 are in units of $j_c\, D$, and we used $d = 2{,}5 \times 10^{-4}\, a$. Notice that J_s and B_η are, respectively, even and odd functions on ζ.

IV Conclusions

We obtained the magnetic response of superconducting bent strips under the influence of external magnetic

or electric fields (the later corresponding to an applied current). A change of coordinates is used in order to transform a two dimensional problem in an one dimensional problem. The sheet current J_s dependence on the coordinate along the strip, ζ, was calculated employing a numerical procedure [12, 14]. In the Meissner state the resulting magnetic field lines correctly show the magnetic shielding bent strips should present. We also compared the flux penetration for bent strips with that for a flat strip. For both the external magnetic field and transport current cases the penetration of magnetic flux from the strips edges, $\zeta = \pm a$, is delayed in bent strips. However, flux penetration from the strip bend, $\zeta = 0$, is observed when a transport current is applied, being more pronounced as α increases.

Acknowledgments

We would like to thank Clécio C. de Souza Silva for helpful discussions. This work was partially supported by Brazilian Science Agencies CNPq and FACEPE.

References

[1] W. T.Norris, J. Phys. D **3**, 489 (1970).

[2] E. H.Brandt and M. Indenbom, Phys. Rev. B **48**, 12893 (1993).

[3] P. N. Mikheenko and Kuzovlev, Physica C **204**, 229 (1993).

[4] J. Zhu, J. Mester, J. Lockhart, and J. Turneaure, Physica C **212**, 216 (1993).

[5] J. R. Clem, R. P. Huebener, and D. E. Gallus,J. Low Temp. Phys. **12**, 449 (1973).

[6] E. H. Brandt and G. P. Miktik, Phys. Rev. Lett. **85**, 4164 (2000).

[7] C. C. S. Silva, L. R. E. Cabral, and J. A. Aguiar, Phys. Rev. B **63**, 4526 (2001).

[8] C. C. S. Silva, L. R. E. Cabral, and J. A. Aguiar, Phys. Status Solidi A **187**, 209 (2001).

[9] E. Zeldov, J. R. Clem, M. McElfresh, and M. Darwin, Phys. Rev. B **49**, 9802 (1994).

[10] G. Blatter, M. V. Feigel'man, V. B. Geshkenbein, A. I. Larkin, and V. M. Vinokur, Rev. Mod. Phys. **66**, 1125 (1994).

[11] E. H. Brandt, Rep. Prog. Phys. **58**, 1465 (1995).

[12] E. H. Brandt, Phys. Rev. B **54**, 4246 (1996).

[13] R. Labusch and T. B. Doyle, Physica C **290**, 143 (1997).

[14] E. H. Brandt, Phys. Rev. B **59**, 3369 (1999).

[15] C. P. Bean, Phys. Rev. Lett. **8**, 250 (1962); *idem*, Rev. Mod. Phys. 36, 31 (1964).

[16] L. R. E. Cabral and J. A. Aguiar, Physica C **341 - 348**, 1049 (2000).